Lidar-based wake tracking for closed-loop wind farm control

Steffen Raach[1], David Schlipf[1], and Po Wen Cheng[1]

[1]Stuttgart Wind Energy (SWE), University of Stuttgart, Allmandring 5B, 70569 Stuttgart, Germany

Correspondence to: Steffen Raach (raach@ifb.uni-stuttgart.de)

Abstract. This work presents two advancements towards closed-loop wake ~~redirecting~~ redirection of a wind turbine. First, a model-based wake tracking approach is presented which uses a nacelle-based lidar system facing downwind to obtain information about the wake. The method uses a reduced order wake model to track the wake. The wake tracking is demonstrated with lidar measurement data from an offshore campaign and with simulated lidar data from a simulation with the Simulator fOr Wind Farm Applications (SOWFA). Second, a controller for closed-loop wake steering is presented. It uses the wake tracking information to set the yaw actuator of the wind turbine to redirect the wake to a desired position. Altogether, the two approaches enable a closed-loop wake redirection.

1 Introduction

In recent years, wind farm control has gained more and more importance in the wind energy control community, ~~since~~ due to interactions between individual wind turbines in a wind farm~~can interact by their flow. The wake interaction can result in less power compared to a fee-stream operation and can result in higher structural load of the downstream turbine due to higher turbulence in the flow and possible partial wake impingements.~~ . The wind speed in the wake of a wind turbine is reduced with respect to the free stream wind speed. Additionally, the turbulence in the wake is increased. If a wind turbine is impacted by a wake from a wind turbine located upwind, the wind turbine produces less power and is faced with higher structural loads because of the increased turbulence, see Borisade et al. (2015). Describing the wake effects and quantifying the decay has been of interest in research for years. Different models have been developed to address different ~~phenomena~~wake properties, such as the velocity deficit and the increased turbulence intensity. There are empirical models, data driven models, and models which describe the physical behavior in the wake, all varying in complexity and computational effort. Mainly, models with low complexity are steady state models which ~~means they~~ describe the interaction in a static manner and no wake propagation is modeled. Further research is needed to develop control oriented dynamic wake models.

The same two goals are valid for both wind turbine and wind farm control: 1) maximization of the total power and 2) reduction of the structural loads. Two main concepts ~~has~~ have been introduced for wind farm control: 1) axial induction control and 2) wake redirection control. Axial induction control aims at manipulating the axial induction by the blade pitch or torque actuator and operating the wind turbine at a lower production level. This results in ~~less of~~ a lower wake deficit and aims at minimizing structural load effects on the downwind wind turbines and preserving energy in the flow~~for downstream turbines~~. The effects on the overall energy capture of the wind farm is not clear yet. Consider Boersma et al. (2017) for a general overview on wind farm control.

The idea of redirecting the wake by the yaw actuator instead of trying to mitigate its intensity has been discussed in different publications, see Fleming et al. (2014a, b); Gebraad et al. (2014). In simulation studies it was shown that the wake is redirected up to 0.54 times the rotor diameter, D, (at a seven ~~diameter~~ D downwind distance) by yawing the turbine up to $40\,\mathrm{deg}$, see Fleming et al. (2014b). Different investigations have shown promising results in improving the power output of a wind farm by applying yaw offsets in open-loop approaches, see Gebraad et al. (2014) and Fleming et al. (2014a). Nevertheless, the form in which it has been applied so far ~~does contain~~ contains drawbacks: 1) Applying optimized yaw angles in a feed-forward approach does not guarantee that the wake is going to the desired direction ~~-~~ and thus, the quality of the model, which is used to compute the yaw angles, highly influences the control performance. 2) There is no observation of whether the wake is being redirected correctly. The concept of closed-loop wake redirection, which was introduced in Raach et al. (2016) ~~,~~ can help to overcome the drawbacks.

A major barrier for wind farm control applications has been the lack of measurement devices to measure the flow interactions between wind turbines, but also ~~their~~ the cost and availability of the devices. Further, modeling the three dimensional flow field is not a straight forward approach since the flow is usually described by the Navier-Stokes equations. Lidar can be a useful tool to address the measurement problem in wind farm applications, while bearing in mind the instrument limitations and the assumptions required to extract the information and exploit the lidar measurement data.

This paper addresses the wind farm control concept of wake ~~redirecting~~redirection. It aims to enable closed-loop wake ~~redirecting~~ redirection by presenting a method to obtain the wake position using lidar measurements. Further, the difficulty in wake position definition and measurability is discussed.

~~First, it presents a~~ A model-based estimation approach is presented and used to obtain important quantities for wake ~~redirecting~~ redirection using a nacelle-based lidar system facing downwind~~. Furthermore,~~, and a closed loop controller is designed and analyzed. In summary, this work presents an entire concept for lidar-based closed-loop wake ~~redirecting~~redirection.

2 Methodology

In order to enable ~~a~~ lidar-based closed-loop wake ~~redirecting~~ redirection within a wind farm, ~~the problem can be divided into~~ two main tasks must be considered: 1) the measurement task and 2) the control task. This work focuses mainly on the measurement task but gives also a summary of a solution to the control task, which was presented in Raach et al. (2016). Figure 1 presents the general concept of ~~the~~ closed-loop wake ~~redirecting~~ redirection and the link between ~~measurement task~~ the measurement and control task.

2.1 Problem formulation for wake-tracking

~~When talking about wake tracking or a wake center position there exists a main problem. There is~~ The main issue in the context of wake tracking algorithms is that no clear definition ~~of~~ exists for the wake center~~, moreover, .~~ Moreover, the idea of a wake

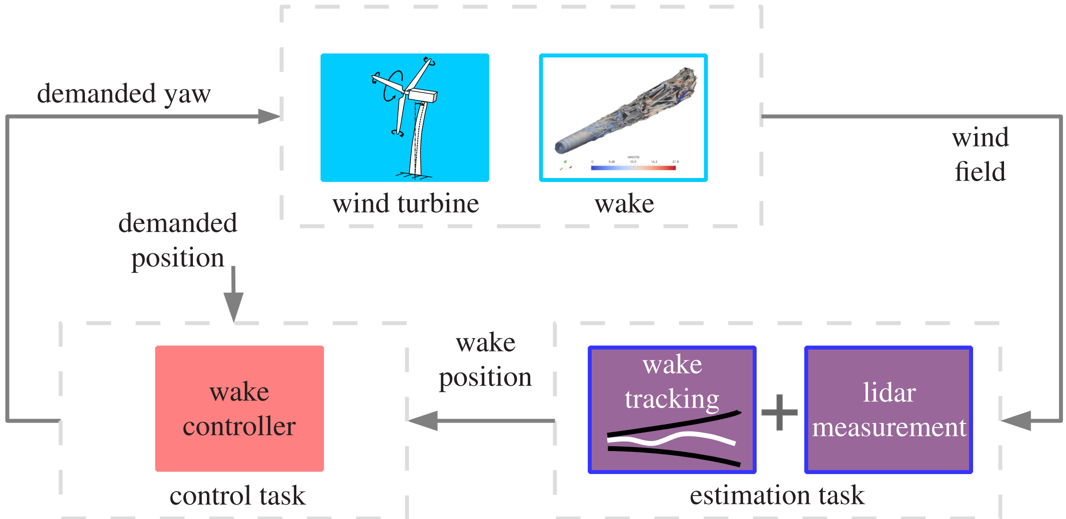

Figure 1. The conceptual idea of closed-loop wake ~~redirecting~~ redirection and its two main tasks: 1) the estimation task addressed in Section 5 and 2) the control task addressed in Section 6.

center is a concept based on time averaged profiles of the wake behind a turbine (1 to 10 minutes averages). Averaging the flow yields a (double) Gaussian function for the velocity deficit profile in the horizontal and vertical directions. From this a wake center can then be defined~~easily~~. However, when different methods are used to define the shape, wake center estimates may ~~be~~ vary under the same flow conditions, see Vollmer et al. (2016). The absence of a unique wake center definition must be considered when comparing results. Furthermore, this means even with full flow field information the wake center is not a measurable quantity and depends on definition.

Consider also Doubrawa et al. (2017) and Howland et al. (2016) for a review of wake center estimation methods. The task of lidar-based wake tracking includes first ~~,~~ a reference definition of the wake center. Then, the result of the estimation method from the lidar measurement data can be compared to the reference definition.

2.2 The estimation task

Measuring flow quantities is crucial for enabling a closed-loop controller to ~~manipulate the wake quantities~~influence the wake properties. The task of the measurement problem is to provide the necessary quantities for the controller. This means using a measurement device, such as a lidar, and processing the measurement data in such a way that they are useful for the controller. Since the lidar measurement principle has several limitations in providing wind field information an adequate estimation technique is used ~~that is~~ as described in Section 5.

2.3 The control task

The second task towards a closed-loop wake redirection is the control task. Its main challenge is to convert the estimated wake position information and ~~the demanded position~~ its desired value to a demanded yaw signal. A feedback controller has to be designed which steers the wake center to the desired position and compensates for uncertainties in the models. Since the reaction of a change in ~~the~~ yaw is measured with a delay due to the wake propagation time, the controller has to be designed ~~in such a way that it can~~ to overcome this limitation.

In the following section, the measurement problem is addressed first. A method is presented to estimate wake information from lidar measurement data using a nacelle-based lidar system. Second, the controller problem is addressed in Section 6. A wake ~~redirecting~~ redirection controller is presented which uses the obtained wake information, (namely the wake center position), and steers the wake ~~center~~ using the yaw actuator~~to a desired position~~. The overall goal of this paper is to ~~also~~ present the framework of lidar-based closed-loop wake redirection ~~with exemplary~~ while providing example models and controller.

3 Reference definition and its impact on the estimation task

In this section the wake center definition is addressed ~~. The comparisons are being performed in simulation since in reality a full flow knowledge is impossible~~through the use of simulation data, which can cover a larger area at a higher spatial and temporal resolution than measurements would be able to provide.

3.1 Wake center definition

As previously mentioned, it is first necessary to define the wake center. The minimum wind power method proposed by Vollmer et al. (2016) is adopted and modified to identify the wake center. Thus, it is defined as the downstream position where a ~~second wind turbine , which orientated identically and has the same rotor diameter than the first,~~ hypothetical turbine of identical characteristics and yaw angle would produce the least power. This yields the minimization problem

$$\min_{y} \int_{0}^{2\pi} \int_{y}^{R+y} u(r,\phi)^3 r \,\mathrm{d}r\mathrm{d}\phi, \tag{1}$$

where the position of the turbine is ~~described in the polar coordinate system (r,ϕ) with the origin~~ at y (lateral offset) and $z = 0$ (hub-height) and the rotor area is described in the polar coordinate system (r,ϕ) . The definition then assumes that the wake center is at (y, z).

The flow field is time averaged over different running window lengths and the impact of the ~~wind~~ window lengths is analyzed. The calculated wake center (at a ~~1.8 diameter~~ $1.8D$ downwind distance) ~~filtered~~ obtained with a running averaged filter with different window lengths are presented in Figure 2. The presented results are for a low turbulence intensity ($TI = 6\%$) SOWFA simulation under a mean hub-height free-stream wind speed ~~$8\,\mathrm{ms}^{-1}$~~ $8\,\mathrm{m/s}$. The available flow field data has a sampling frequency of $1\,\mathrm{Hz}$ and the wake center is calculated from each sample. The wake center clearly converges to a steady value with

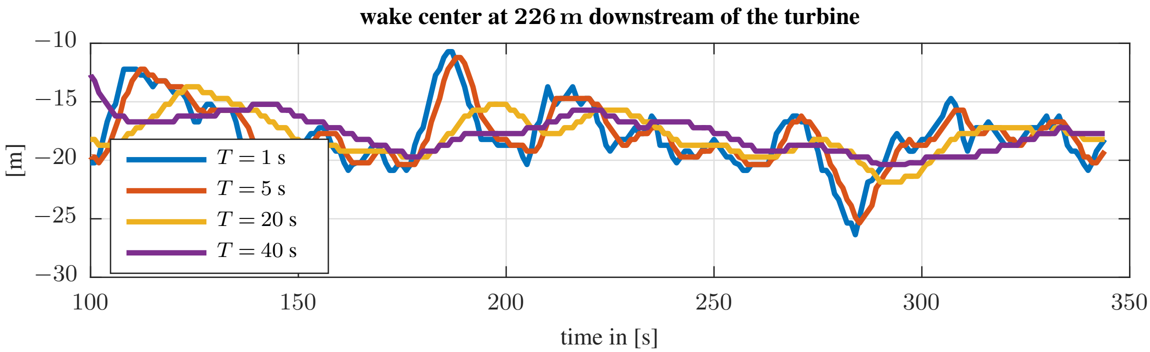

Figure 2. Time evolution of wake center (at a ~~1.8 diameter~~ $1.8D$ downwind distance) when different window lengths T are used to average the flow during the wake center calculation.

increasing averaging time T. An increased averaging time, however, slows the adjustment, e.g. to a changing wind direction, or a set point change, and should be considered when choosing an averaging time.

3.2 Problem discussion of lidar-based wake tracking

~~Compared to other problems in lidar-based wind field reconstruction the~~ The problem of wake center estimation is different from other problems in lidar-based wind field reconstruction. Other model based approaches in wind field reconstruction (e.g. estimation of the rotor-effective wind speed, or of u and v wind vector components using lidar measurements as in Schlipf et al. (2012)) can first be compared to existing quantities. Further, the models can be used to predict line-of-sight velocities (v_{los}) of lidar measurements and be directly compared to the real data. Therefore, the model can be used in two directions, estimating and predicting the wind field.

~~Here, having~~ When the wake center ~~defined like~~ is defined as in Eq. (1) the prediction of the wind field from a given position is not possible and ~~further~~ neither is a direct comparison of line-of-sight data~~is not possible~~. Nevertheless, the wake center position definition ~~seems to be very convenient and is therefore used as reference.~~ is used as a reference because of its robustness and simplicity.

4 A simplified wake model for wake tracking

The estimation task addresses the processing and estimation of useful information and provides them to the controller. Since a lidar system has several limitations, the desired quantities ~~,~~ like the wake position ~~,~~ or the wake deficit, are not directly measurable and have to be estimated from the measurement data. One main limitation of ~~a lidar system is that it only~~ wind lidar systems is that they returns the projection of the wind speeds along the direction of the laser beam. This means that a lidar system only provides scalar information of the actual wind vectors. Further, the wind speed is not measured at a certain point but in a volume around the desired measurement location. A solution to these limitations is to implement model-based wind field reconstruction. Wind field reconstruction methods have been developed and used for different applications of lidar systems in wind energy, for example static two- and three-dimensional, Schlipf et al. (2012), dynamic three dimensional wind field reconstruction methods, Raach et al. (2014), ~~and~~ approaches for floating lidar systems, Schlipf et al. (2012), and also for wake measurements Lundquist et al. (2015). Here, the concept of wind field reconstruction is used to obtain information about the wake.

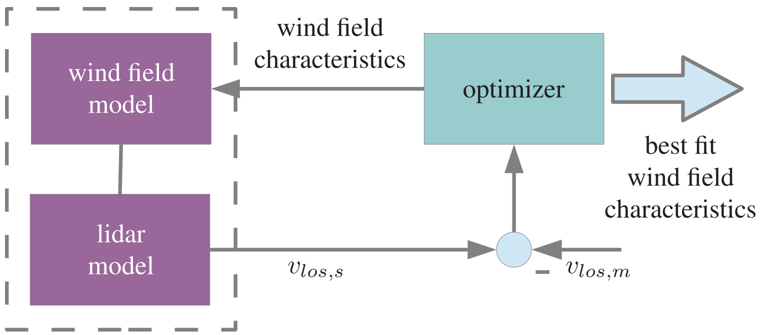

Figure 3. The general concept of model-based wind field reconstruction, in which the wind field characteristics are estimated by fitting simulated lidar measurement data ($v_{los,s}$) to measurements ($v_{los,m}$).

The general approach of wind field reconstruction from lidar data is to estimate wind field characteristics from an internal model by fitting simulated lidar data to the measured ones. In Figure 3 the basic idea of model-based wind field reconstruction is shown. An optimizer is used to find the best fit for a model of the assumed wind field with the defined lidar configuration. The optimizer minimizes the square error of the modeled (simulated) $v_{los,s}$ and the measured $v_{los,m}$ lidar line-of-sight velocities and returns the estimated model parameter (e.g. wake center position, wake decay, wake deficit, etc.).

In this work, a lidar and a wind field model is used. The wind field model consists of a background wind field model, which defines the ambient wind speed and its profile, and a wake model. The wake model includes the main wake effects: wake deficit, wake evolution, and wake center displacement. The models are presented in the following section.

4.1 Wind field model

Figure 4 shows the subparts of the wind field model: 1) the underlaying wind field, and 2) the wake model.

The wind field model is described in a wind coordinate system which is denoted by the subscript W. It is rotated horizontally with respect to the global inertial coordinate system I and aligned with the wind direction. The wind speed vector in the W-system is transformed in the I-system by

$$\begin{bmatrix} u \\ v \\ w \end{bmatrix}_I = \begin{bmatrix} \cos\alpha & -\sin\alpha & 0 \\ \sin\alpha & \cos\alpha & 0 \\ 0 & 0 & 1 \end{bmatrix} \begin{bmatrix} u \\ v \\ w \end{bmatrix}_W , \tag{2}$$

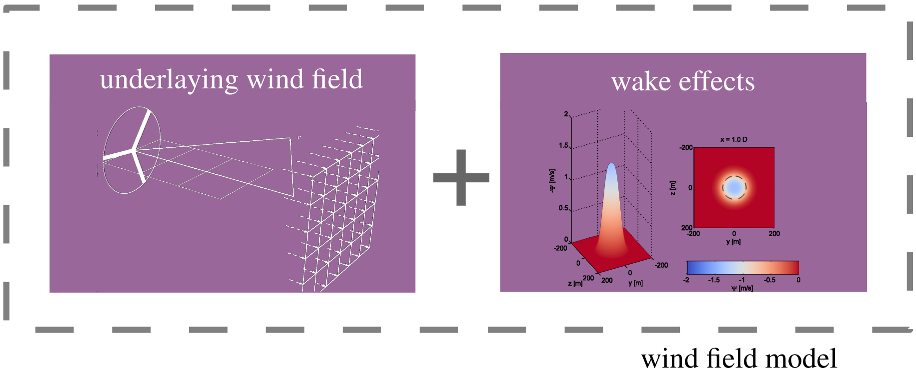

Figure 4. The submodels of the wind field model (in the wind coordinate system W): 1) the underlaying wind field, and 2) the wake model.

where α is the horizontal rotation of the wind field. The underlying wind field includes the rotor effective wind speed v_0 and vertical linear shear δ_V. It is assumed that the wind field has only a u component. Thus, in the W coordinate system, the underlying wind field vector at point i with the coordinates $\left[x_i, y_i, z_i\right]^T$ is

$$\begin{bmatrix} u \\ v \\ w \end{bmatrix}_{i,W} = \begin{bmatrix} v_0 + z_i \delta_V \\ 0 \\ 0 \end{bmatrix}, \tag{3}$$

where z_i is the height above the ground. This is illustrated in Figure 4 on the left. Further, the wind field is linearly overlaid with the wake model Ψ for the u and v components yielding

$$\begin{bmatrix} u \\ v \\ w \end{bmatrix}_{i,W} = \begin{bmatrix} v_0 + z_i \delta_V + \Psi_{u,i} \\ \Psi_{v,i} \\ 0 \end{bmatrix}. \tag{4}$$

In the following section, the considered wake effects are described and the wake model is presented.

4.1.1 Wake deficit and wake evolution model.

~~The rotor extracts energy from the wind and converts it into electrical energy. Therefore, the wind speed is reduced behind a wind turbine. Through mixing and energy flow from the surrounding the momentum deficit recovers.~~ The wake deficit is modeled with an initial wake deficit at the rotor disk with tip and root losses depending on the energy extraction. In order to get the initial deficit, the energy extraction is mapped by applying Prandtl's root and tip loss function Γ_{Prandtl}. Applying the energy conservation assumption yields

$$(v_0 + s\Gamma_{\text{Prandtl}})^2 - (1 - c_P)v_0 = 0, \tag{5}$$

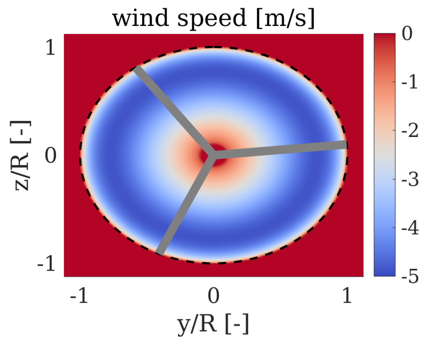

Figure 5. The initial wake deficit directly evaluated at the rotor (at $0\,\mathrm{m}$ downstream). The mean hub-height wind speed ~~($8\,\mathrm{ms}^{-1}$)~~ ($8\,\mathrm{m/s}$) was removed for simplicity. No yaw misalignment is applied.

with the power coefficient c_p. Solving this equation for s gives the initial wake deficit

$$\Psi_{\text{init}} = s_{\text{solution}} \Gamma_{\text{Prandtl}}. \tag{6}$$

An ~~exemplary~~ example initial wake deficit Ψ_{init} is shown in Figure 5.

The wake ~~is evolving~~ evolves as it moves away from the wind turbine. ~~New energy~~ Energy flows in from the freestream and mixes with the wake. ~~Physically these dynamics are described via the~~ The Navier-Stokes equations ~~. These are partial differential equations and it~~ describe the flow behavior, however, because of the nonlinearities using them would be a ~~very complex taskto estimate the wake using these equations. However, here~~ complex task. Here, an empirical model is used which models the wake recovery. However, in contrast to other wake models, the wake evolution is modeled by a Gaussian shape ~~2D~~ two-dimensional filter. The ~~2D~~ two-dimensional filter Ξ depends on the distance d behind the wind turbine

$$\Xi(d, y_i, z_i) = \exp\left(\frac{y_i^2 + z_i^2}{2\sigma_f^2(d)}\right) \tag{7}$$

with

$$\sigma_f(d) = \frac{d \cdot \epsilon}{2\sqrt{2\log(2)}} \tag{8}$$

and y_i and z_i the grid points in distance d. With the parameter ϵ the dissipation rate can be set.

Thus, for every distance behind the rotor, the wake can be evaluated using the initial wake deficit Ψ_{init} and the filter (7). The wake deficit results from the convolution of the initial wake deficit Ψ_{init} with the filter $\Xi(d, y_i, z_i)$ to

$$\Psi(d, y_i, z_i) = \Xi(d, y_i, z_i) * \Psi_{\text{init}} \tag{9}$$

4.1.2 Wake deflection model.

The wake deflection caused by a yaw misalignment γ is additionally modeled. The relationship is derived in the study of Jiménez et al. (2010) and was successfully used in an optimization of the yaw angles for a simulated wind farm in Gebraad et al. (2014). The angle of the wake with respect to the main wind direction is

$$\xi(d, c_T, \gamma) = \frac{\xi_{\text{init}}(c_T, \gamma)}{\left(1 + \beta \frac{d}{D}\right)^2}, \tag{10}$$

with the initial angle of the wake at the rotor

$$\xi_{\text{init}}(c_T, \gamma) = \frac{1}{2} \cos^2(\gamma) \sin(\gamma) c_T \tag{11}$$

and model parameter β, which defines the sensitivity of the wake deflection to yaw and is here assumed to be known in advance. Further, c_T is the thrust coefficient and D the rotor diameter. Further, the yaw induced deflection at the downwind position d is according to Gebraad et al. (2014)

$$\delta_{\text{yaw}}(d, c_T, \gamma) = -\xi_{\text{init}}(c_T, \gamma) \frac{D}{30\beta} \left[15 \left(1 - \frac{1}{1 + \frac{2\beta d}{D}} \right) + \xi_{\text{init}}(c_T, \gamma)^2 \left(1 - \frac{1}{\left(1 + \frac{2\beta d}{D}\right)^5} \right) \right]. \tag{12}$$

The rotation is applied to the wake deficit and yields a u and v component of the wake model,

$$\begin{bmatrix} \Psi_{u,i} \\ \Psi_{v,i} \\ 0 \end{bmatrix}_W = \begin{bmatrix} \cos\xi(d, c_T, \gamma) & -\sin\xi(d, c_T, \gamma) & 0 \\ \sin\xi(d, c_T, \gamma) & \cos\xi(d, c_T, \gamma) & 0 \\ 0 & 0 & 1 \end{bmatrix} \begin{bmatrix} \Psi_i \\ 0 \\ 0 \end{bmatrix}_W . \tag{13}$$

In Figure 6 two different wake situations are shown ~~, the~~ for $\gamma = 0\,\text{deg}$ and $\gamma = 25\,\text{deg}$. The first is a non-yawed case and in the second case the turbine is yawed with ~~$\gamma = 25\,\text{deg}$~~ $25\,\text{deg}$. In both cases the ~~underlying~~ underlaying wind field has a mean hub-height free stream wind speed of $v_0 = 16\,\text{m/s}$ and no vertical shear.

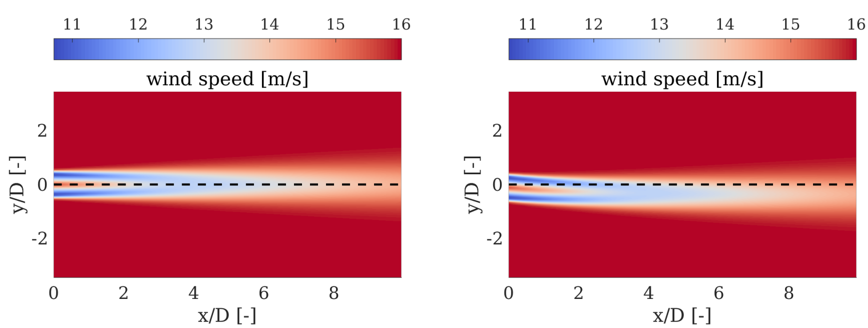

(a) Non-yawed case.

(b) Turbine is yawed with $\gamma = 25\,\text{deg}$.

Figure 6. Visualization of two wake situations within a constant wind field of $v_0 = 16\,\text{m/s}$, axial induction $a = 0.15$ and dissipation rate $\epsilon = 0.1$.

5 The estimation task - model-based wake tracking

As summarized before, the estimation task ~~performs the wake tracking~~ tracks the wake using the presented wake model. To perform ~~a~~ lidar-based waked tracking a lidar model is needed. First, the lidar model is presented and then the wake tracking approach is described. Finally, estimation results of two different cases are presented and discussed.

5.1 Lidar model

The lidar measurements can be modeled by a point measurement in the wind field. In the inertial coordinate system this is done by a projection of the wind vector $\begin{bmatrix} u_i & v_i & w_i \end{bmatrix}_I^T$ onto the normalized laser vector in the i-th point $\begin{bmatrix} x_i & y_i & z_i \end{bmatrix}_I^T$ with focus distance $f_i = \sqrt{x_{i,I}^2 + y_{i,I}^2 + z_{i,I}^2}$ by

$$v_{los,i} = \frac{x_{i,I}}{f_i} u_{i,I} + \frac{y_{i,I}}{f_i} v_{i,I} + \frac{z_{i,I}}{f_i} w_{i,I}. \tag{14}$$

5.2 Model-based wake tracking

As depicted in Figure 3, the model based wind field reconstruction method estimates the model parameter by minimizing the error between measured line-of-sight wind speed $v_{los,m}$ and simulated line-of-sight wind speed $v_{los,s}$. A nonlinear optimization problem is formed for n measurement points. This yields

$$\min_p f(x) = \min_p \begin{bmatrix} (v_{los,m,1} - v_{los,s,1})^2 \\ \vdots \\ (v_{los,m,n} - v_{los,s,n})^2 \end{bmatrix}, \tag{15}$$

where in p all free model parameters are included. The free model parameters are listed in Table 1. An example of an estimation step of the wake tracking from a measurement campaign at the alpha ventus offshore wind farm is shown in Figure 7.

5.3 Evaluation and discussion

Figure 7 ~~shows that the model fits well for the application and can be applied with real~~ confirms the applicability of the method with lidar measurement data. In the following, SOWFA (Churchfield and Lee (2012)) is ~~considered~~ used as simulation tool. Flow snapshots of ~~a simulation~~ simulations of a single wind turbine are stored. The flow field is then scanned with a lidar

Table 1. The free model ~~parameter~~ parameters for the wind field model which are estimated in the optimizer.

underlaying wind field	
v_0	rotor effective wind speed
δ_V	vertical linear shear

wake model	
c_T	thrust coefficient
c_P	power coefficient
γ	turbine yaw angle
ϵ	wake dissipation coefficient

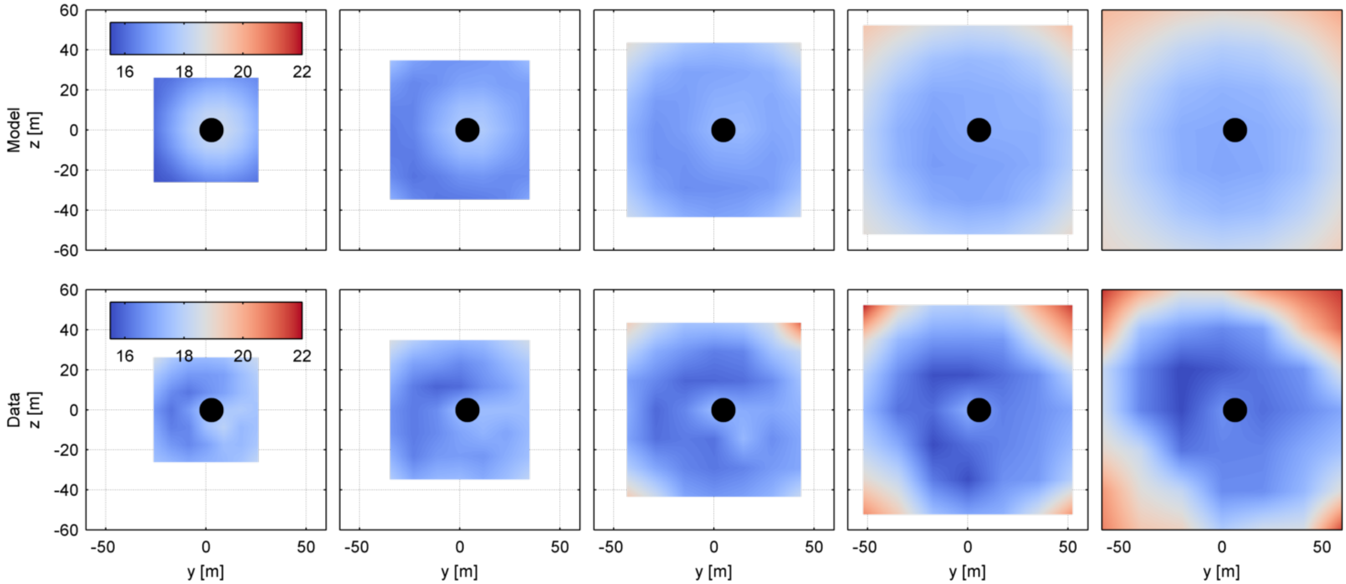

Figure 7. An ~~exemplary~~ example estimation step of the wake tracking. The simulated lidar measurements in the first row are compared to the measured lidar data in the second row for five downstream distances from 0.6 to 1.4 ~~times the rotor diameter~~ D (from left to right, [0.6, 0.8, 1.0, 1.2, 1.4], looking downstream). The estimated wake center is marked with the black dot.

simulator. The lidar scans with a 7×7 grid at five distances from ~~0.6 to 1.4 times the rotor diameter (~~$0.6D$ to $1.4D$ (with $D = 126\,\mathrm{m}$). Two different cases are analyzed~~: First, a casewhere the turbine is aligned with~~. In the first case, the turbine rotor is perpendicular to the wind direction ~~. The estimation~~ ($\gamma = 0\,\mathrm{deg}$) and these results are shown in Figure 8. ~~Second, the turbine is misaligned with~~ In the second case, the yaw misalignment is $30\,\mathrm{deg}$ ~~to deflect the wake~~ so that the wake is deflected. The results of the wake tracking ~~is~~ are shown in Figure 9. In both figures the wake center is estimated at the furthest scanning distance of $1.4D = 176.4\,\mathrm{m}$. In both cases the method shows the ability ~~of estimating~~ to estimate the wake parameter and tracking ~~the wake~~ its center.

As mentioned before the wake center position needs to be calculated using a specific definition and there is no direct measurable representation of it. In Figure 10 the lidar-based wake tracking is compared to the wake center estimation using the definition of Eq. (1) without any filtering.

6 The control task

The following closed-loop controller was first presented in Raach et al. (2016) and is recapped here. Consider also Raach et al. (2017) where a $\mathcal{H}_\infty$ controller design for closed-loop wake redirection with defined performance margins.

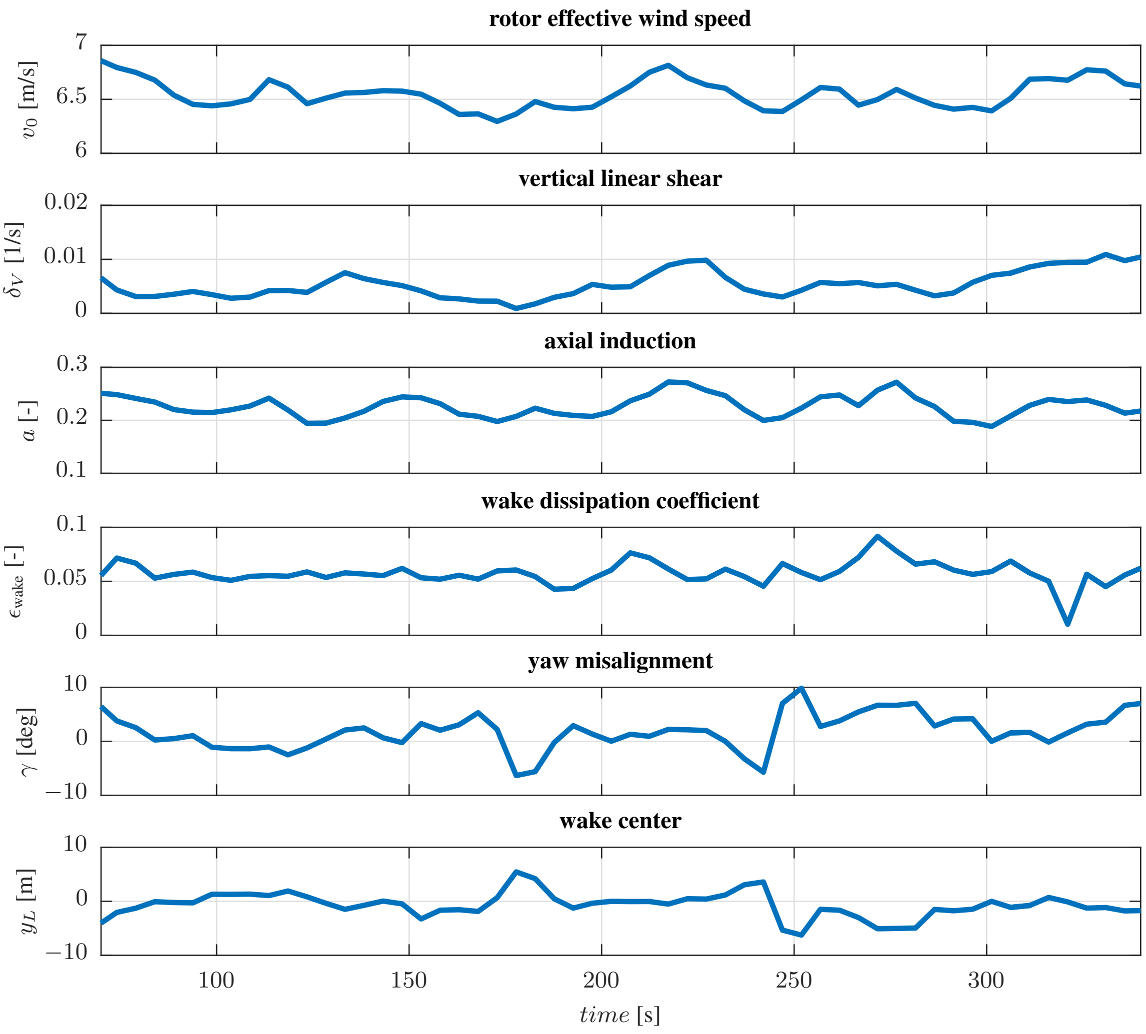

Figure 8. Time results of the wake tracking of a SOWFA simulation. The wind turbine is aligned with the ~~main~~ mean wind direction. The lidar scanned in a 7×7 grid at five distances from $0.6D$ to $1.4D$. The wake center is estimated at the furthest scanning distance $1.4D = 176.4\,\mathrm{m}$.

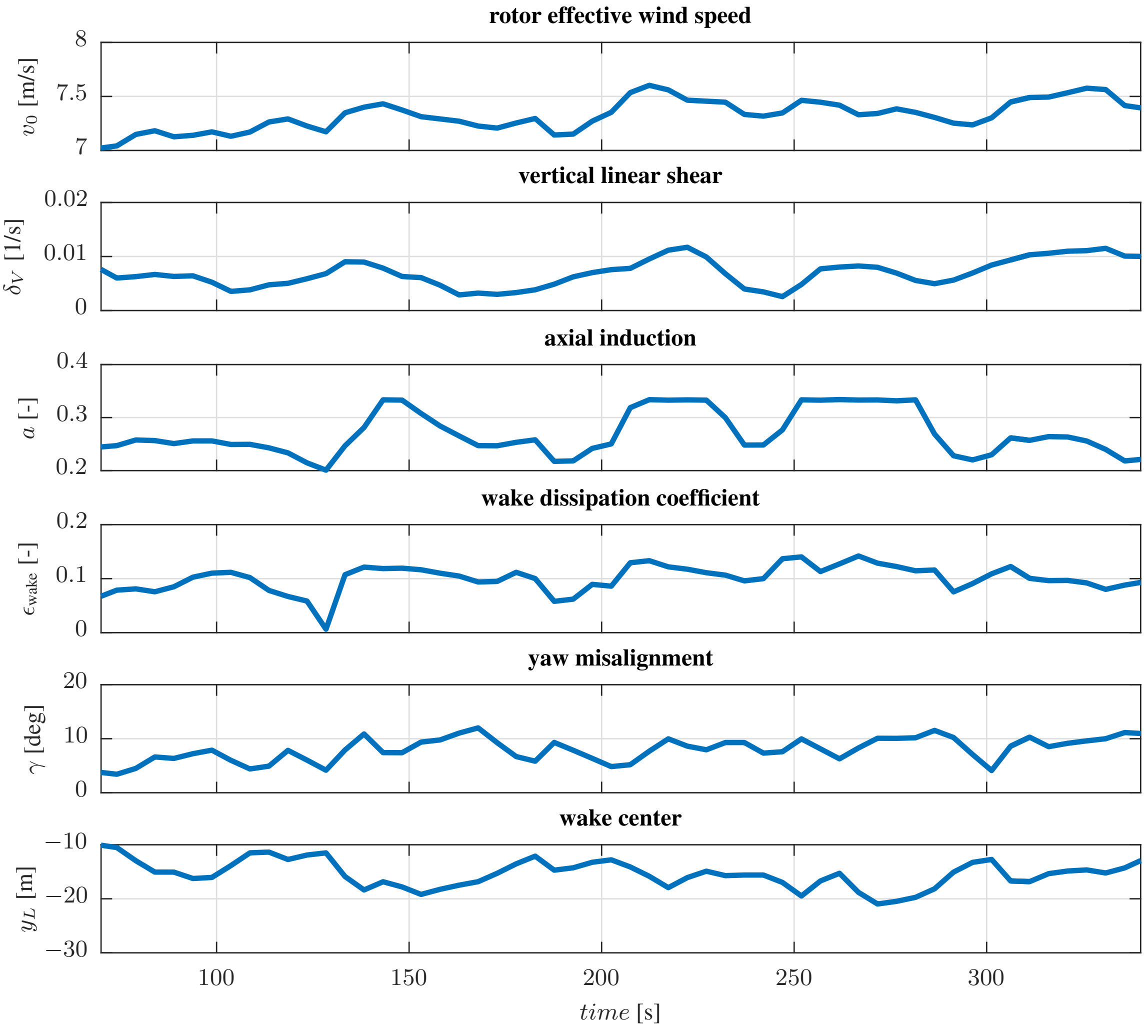

Figure 9. A second time evolution of the different estimated wind field and wake quantities. In this case, the wind turbine is misaligned with 30 deg and the wake is deflected. The lidar scanned in a 7×7 grid at five distances from $0.6D$ to $1.4D$. The wake center is estimated at the furthest scanning distance $1.4D = 176.4\,\mathrm{m}$.

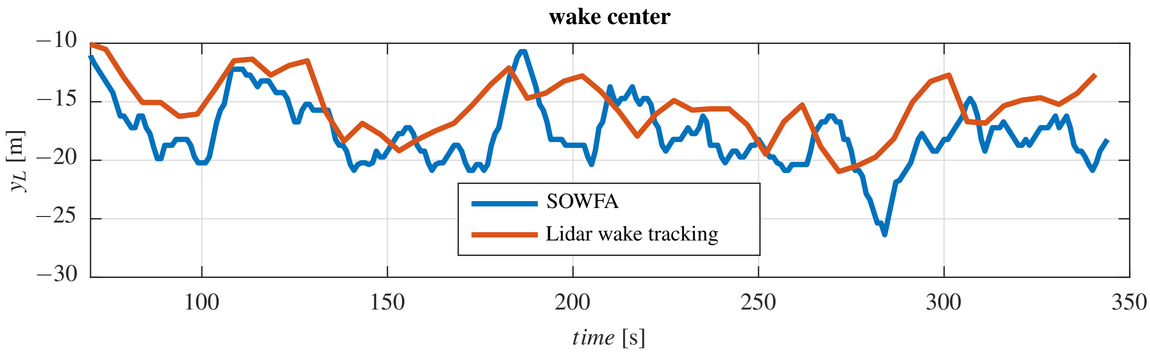

Figure 10. Comparison between the wake center estimation (see Eq. (1)) and the lidar-based wake tracking method.

As mentioned above, the reaction of the wake to a yaw action can only be measured with a time delay. To control a delayed system, the Smith Predictor approach, which is based on internal model control, has been derived and used in many applications. ~~Internal model control is the basic idea of a Smith Predictor.~~

The presented controller follows the idea of internal model control in which the difference between the actual system output and a predicted output is used within the controller to regulate the system. Therefore, a model is necessary for describing the wake effects in a simplified but sufficient way. It consists of ~~the controller which is a classical~~ a proportional-integral (PI) controller. Further, an internal model is used which approximates the real system behavior. The wake propagation which exists because the wake flow has to evolve until it reaches the measurement location of the lidar system is ~~approximated with a~~ modeled using a time delay. The ~~time delay~~ delay time τ varies with respect to the mean wind speed. Finally, a filter is needed to cancel out controller actions which can not be observed because of the time difference between control action and measurement location. Figure 11 shows the general concept of the controller.

6.1 Internal wake model of the controller

As depicted in ~~Fig.~~ Figure 11, the wake controller needs an internal model to predict the reaction of the wake to the demanded yaw angle. The internal wake model includes the yaw actuator and the ~~yaw induces~~ gain between the yaw and the wake deflection. For the wake model the assumptions of a constant ~~thrust coefficient~~ c_T is made. Altogether, this yields an internal controller model $\widetilde{\Psi}$ of the reality Ψ:

$$\widetilde{\Psi}: \left\{ \begin{array}{rcl|l} & & \ddot{\gamma} + 2d\omega\dot{\gamma} + \omega^2\gamma = \omega^2\gamma_{dem} & \text{yaw actuator dynamic} \\ \tilde{y} & = & \delta_{\text{yaw}}(d_{\text{Lidar}}, c_{T,\text{const}}, \gamma) & \text{wake deflection model} \end{array} \right. \tag{16}$$

with γ_{dem} the demanded yaw angle and d_{Lidar} the distance to the measurement location.

There is a time delay because the wake first needs to evolve to the measurement location:

$$\tilde{y}_L(t) = \tilde{y}(t - \tau). \tag{17}$$

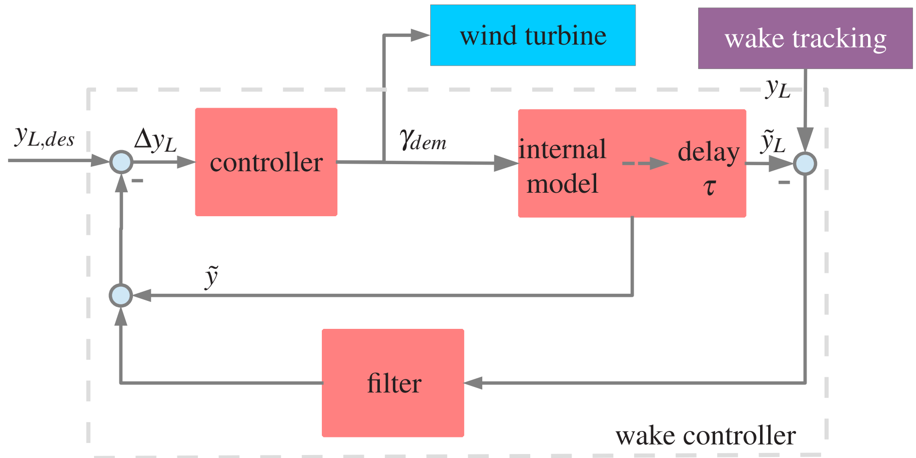

Figure 11. The general structure of the wake steering controller: The controller, a simplified wake model and the wake propagation modeled with a delay, and the filter. The controller uses the difference, δy_L, between the predicted output $\tilde{y}$, the measured output y_L and the desired output $y_{L,des}$ to set the demanded yaw angle γ_{dem}.

For the controller design, the time delay is approximated using the Padé approximation of time delays, see Skogestad and Postlethwaite (2005).

6.2 Controller design

The primal goal of the wake controller is to steer the wake center to a desired point in a defined distance by yawing the wind turbine. As mentioned, this is done using a Smith Predictor, which uses an internal model to predict the output reaction. Then the predicted wake center position and the filtered error between predicted and measured wake center position is fed back to the controller.

6.2.1 Controller

A standard ~~proportional-integral (PI)~~ PI controller is used. It is designed such that the closed-loop performance with the internal model (16) meets a phase margin of $60\,\mathrm{deg}$ and a closed-loop bandwidth of $\omega_{\mathrm{CL}} = \frac{1}{2\tau}$. This yields a controller of the form

$$u = K_p\left(\Delta y_L + \frac{1}{T_i}\int \Delta y_L \mathrm{d}t\right), \tag{18}$$

with the proportional gain K_p~~and~~, the time constant T_i, and the error between desired and actual wake center position Δy_L.

6.2.2 Filter

The wake propagation and the caused delay ~~disables a direct measure~~ precludes direct measurement of a yaw change and because of that one has to filter the measured feedback to prevent non-observable yaw actions. Since the delay τ is time varying and depends on the mean wind speed the filter has to be adaptable. Therefore, the cutoff frequency of the butterworth low-pass filter is set to $\omega_{\text{filter}} = \frac{\pi}{8\tau}$.

6.3 Evaluation and discussion

In the following the wake controller is analyzed. Further, the sensitivity~~and~~ , the complementary sensitivity and the controller sensitivity of the closed-loop system is assessed. ~~Consider Skogestad and Postlethwaite (2005)for a detailed~~ Considering Skogestad and Pos the sensitivity gives the closed-loop transfer function from the output disturbance to the output while the complementary sensitivity is the closed-loop transfer function from the reference to the output. The controller sensitivity gives the closed-loop transfer function from the output disturbance to the controller. For more details and a description on controller design and analysis we refer to Skogestad and Postlethwaite (2005).

6.3.1 Controller analysis

In the following, the transfer function of the wake controller is assessed. As shown in Figure 11 the wake controller consists of the internal controller C, an internal model $\widetilde{\Psi}$, the time delay approximation W and the filter F. Having merged all parts the wake controller K is

$$K = \frac{F}{(1 + C\Psi(1 - FW))}. \tag{19}$$

Figure 12 shows the bode analysis of the wake controller K. The controller shows integration behavior, starting with $-90\,\text{deg}$ phase.

6.3.2 Closed-loop analysis

To perform closed-loop analysis the internal controller model $\widetilde{\Psi}$ is transformed to Laplacian space yielding the plant G. Then, the sensitivity S~~and~~ , the complementary sensitivity T~~that are~~ , and the controller sensitivity U that are

$$S = \frac{1}{1 + GK} \tag{20}$$

$$T = \frac{GK}{1 + GK}, \tag{21}$$

$$U = \frac{K}{1 + GK}, \tag{22}$$

with the controller K are assessed and shown in Figure 13. The sensitivity shows a disturbance attenuation up to the controller bandwidth $\omega_{\text{CL}} = 0.02\,\text{Hz}$. Further, the controller sensitivity has low gain for high frequencies. This means the controller does not react on high frequency disturbances.

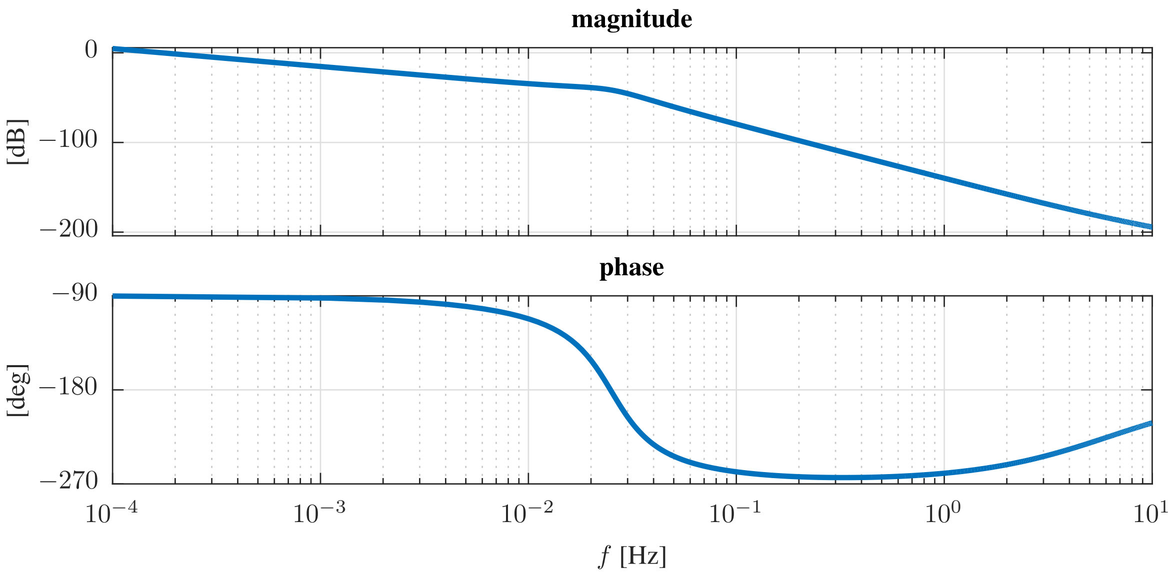

Figure 12. Bode analysis of the designed controller K.

7 Conclusions

This paper introduces first a method which uses lidar measurements to estimate wind field parameters and enables a tracking of the wake center position. Second, a controller is presented which uses this information to redirect the wake to a desired position. In two different cases using simulated lidar measurements of SOWFA simulations, the wake tracking shows promising results in estimating the wake center. The difficulty in wake center position definition is elaborated. A definition is used and the wake tracking results are compared to it. The challenges of a lidar-based wake ~~redirecting~~ redirection control problem are discussed and an appropriate controller is designed to meet the desired requirements. This enables the next step towards ~~a~~ closed-loop wake ~~redirecting~~ redirection in a high fidelity simulation tool~~which is aimed as a next step.~~.

~~As an outlook, the~~ The presented framework of lidar-based closed-loop wake steering offers new possibilities for wind farm control. In ~~a~~ the future, a balance between measuring the near wake, which will result in a higher controller bandwidth, and in the far wake, which will give more reliable information on the wake direction, needs to be found. In a next step, it will be implemented and tested in a high fidelity simulation tool and tested in real time. For the control problem robust controllers will be investigated. Dynamic estimation techniques as well as other wake estimation models will be used for comparing the ability of tracking the wake and finding the most suitable approach for this task.

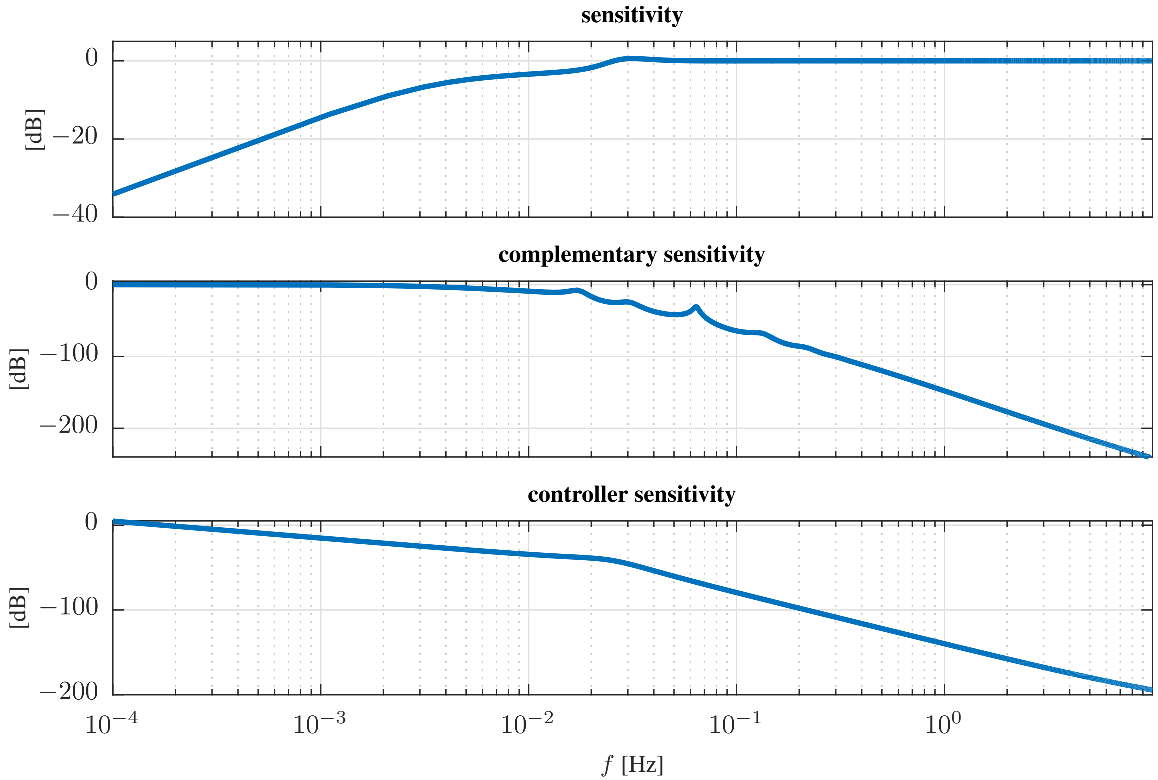

Figure 13. Sensitivity S~~and~~, complementary sensitivity T, and controller sensitivity U analysis of the closed-loop system.

References

Boersma, S., Doekemeijer, B., Gebraad, P., Fleming, P.and Annoni, J., Scholbrock, A., Frederik, J., and van Wingerden, J.-W.: A Tutorial on Control-Oriented Modeling and Control of Wind Farms, in: Proceedings of the American Control Conference (ACC), 2017.

Borisade, F., Luhmann, B., Raach, S., and Cheng, P. W.: Shadow Effects in an Offshore Wind Farm - Potential of Vortex Methods for Wake Modelling, in: Proceedings of the German Wind Energy Conference DEWEK, Bremen, Germany, 2015.

Churchfield, M. and Lee, S.: NWTC design codes-SOWFA, URL: http://wind.nrel.gov/designcodes/~~simulator s~~simulators/SOWFA, 2012.

Doubrawa, P., Barthelmie, R. J., Wang, H., and Churchfield, M. J.: A stochastic wind turbine wake model based on new metrics for wake characterization, Wind Energy, 20, 449–463, doi:10.1002/we.2015, http://dx.doi.org/10.1002/we.2015, 2017.

Fleming, P., Gebraad, P. M., Lee, S., Wingerden, J.-W., Johnson, K., Churchfield, M., Michalakes, J., Spalart, P., and Moriarty, P.: Simulation comparison of wake mitigation control strategies for a two-turbine case, Wind Energy, 18, 2135–2143, 2014a.

Fleming, P. A., Gebraad, P. M., Lee, S., van Wingerden, J.-W., Johnson, K., Churchfield, M., Michalakes, J., Spalart, P., and Moriarty, P.: Evaluating techniques for redirecting turbine wakes using SOWFA, Renewable Energy, 70, 211–218, 2014b.

Gebraad, P. M. O., Teeuwisse, F. W., van Wingerden, J., Fleming, P., Ruben, S. D., Marden, J. R., and Pao, L. Y.: Wind plant power optimization through yaw control using a parametric model for wake effects—a CFD simulation study, Wind Energy, 19, 95–114, doi:10.1822/we, 2014.

Howland, M. F., Bossuyt, J., Martinez-Tossas, L. A., Meyers, J., and Meneveau, C.: Wake Structure of Wind Turbines in Yaw under Uniform Inflow Conditions, http://arxiv.org/abs/1603.06632, arXiv:1603.06632 [physics], 2016.

Jiménez, Á., Crespo, A., and Migoya, E.: Application of a LES technique to characterize the wake deflection of a wind turbine in yaw, Wind Energy, 13, 559–572, 2010.

Lundquist, J. K., Churchfield, M. J., Lee, S., and Clifton, A.: Quantifying error of lidar and sodar Doppler beam swinging measurements of wind turbine wakes using computational fluid dynamics, Atmospheric Measurement Techniques, 8, 907–920, doi:10.5194/amt-8-907-2015, 2015.

Raach, S., Schlipf, D., Haizmann, F., and Cheng, P. W.: Three Dimensional Dynamic Model Based Wind Field Reconstruction from LiDAR Data, in: Journal of Physics: Conference Series: The Science of Making Torque From Wind, vol. 524, Copenhagen, Denmark, 2014.

Raach, S., Schlipf, D., Borisade, F., and Cheng, P. W.: Wake redirecting using feedback control to improve the power output of wind farms, in: Proceedings of the American Control Conference (ACC), Boston, USA, 2016.

Raach, S., van Wingerden, J.-W., Boersma, S., Schlipf, D., and Cheng, P. W.: Hinf controller design for closed-loop wake redirection, in: Proceedings of the American Control Conference (ACC), 2017.

Schlipf, D., Rettenmeier, A., Haizmann, F., Hofsäß, M., Courtney, M., and Cheng, P. W.: Model Based Wind Vector Field Reconstruction from Lidar Data, in: Proceedings of the German Wind Energy Conference DEWEK, Bremen, Germany, 2012.

Skogestad, S. and Postlethwaite, I.: Multivariable Feedback Control: Analysis and Design, John Wiley & Sons, 2005.

Vollmer, L., Steinfeld, G., Heinemann, D., and Kühn, M.: Estimating the wake deflection downstream of a wind turbine in different atmospheric stabilities: an LES study, Wind Energy Science, 1, 129–141, doi:10.5194/wes-1-129-2016, 2016.